

Controllable electron spin dephasing due to phonon state distinguishability in a coupled quantum dot system

Michał Gawelczyk,^{1,2,*} Mateusz Krzykowski,² Krzysztof Gawarecki,² and Paweł Machnikowski²

¹*Department of Experimental Physics, Faculty of Fundamental Problems of Technology, Wrocław University of Science and Technology, Wybrzeże Stanisława Wyspiańskiego 27, 50-370 Wrocław, Poland*

²*Department of Theoretical Physics, Faculty of Fundamental Problems of Technology, Wrocław University of Science and Technology, Wybrzeże Stanisława Wyspiańskiego 27, 50-370 Wrocław, Poland*

We predict a spin pure dephasing channel in a spin-preserving electron tunneling between quantum dots in external magnetic field. The dephasing does not rely on any spin-environment coupling and is caused by a mismatch in g -factors in the two dots leading to distinguishability of phonon packets emitted during tunneling with opposite spins. Combining multiband $\mathbf{k} \cdot \mathbf{p}$ modeling and dynamical simulations via a Master equation we show that this fundamental effect of spin measurement effected by the phonon bath may be controlled by size and composition of the dots or by external fields. By comparing the numerically simulated degree of dephasing with the predictions of general theory based on distinguishability of environment states we show that the proposed mechanism is the dominating phonon-related spin dephasing channel in the system.

PACS numbers: 85.75.-d, 03.65.Yz

Coherence of quantum superpositions distinguishes quantum systems from classical ones and can be exploited in information processing protocols beyond the classical computation schemes [1]. As quantum coherence is extremely fragile, much effort has been invested in understanding and quantifying its effects as well as in the search for methods of reducing or controlling its impact. The paradigmatic model of genuinely quantum decoherence, that has no classical counterpart, is the pure dephasing due to build-up of correlations with the environment (which is equivalent to information transfer from the system to the outside world). In such a process, the quantum nature of the state (or of the information it contains) is destroyed without affecting the probabilities of finding the system in a given basis state (the classical part of the information). The discussion of this effect goes back to the celebrated complementarity between the coherence of paths and the knowledge on which of them the particle has chosen in a double-slit interference experiment [2, 3], hence the term *which way* decoherence. Such process is fundamental in our understanding of quantum measurement and emergence of classicality [4, 5].

Apart from their general importance, dephasing processes are critical for coherent control of quantum states aimed at applications in quantum information [6, 7] and spintronics [8–11]. Dephasing analogous to the *which way* decoherence appears in every quantum system in which the reservoir response to the system dynamics depends on its quantum state [3, 12, 13]. For instance, spin initialization in a quantum dot (QD) can be achieved by spin-preserving tunneling, leading to exciton dissociation [14–18]. This process can be relatively fast, preventing the comparatively slow spin flip processes from perturbing it. However, we have recently found, using a simple model, that *which way* spin decoherence may affect spin states in the exciton dissociation in a magnetic field [19].

The effect does not rely on any direct or spin-mixing-induced spin-environment interaction and is exclusively due to a misfit between electron g -factors, and hence Zeeman splittings, in the two QDs. This results in different tunneling transition energies for the two spin orientations and leads to a *which way* dephasing process, where the phonon bath “measures” the spin state of the tunneling electron via the energy of the emitted phonon. Hence, even though spins confined in QDs offer long spin life times [20] and, under certain conditions, coherence times [21], the *which way* dephasing limits the fidelity of spin initialization.

In this Letter we combine the general ideas of *which way* dephasing with accurate modeling of the quantum states and dynamics of a semiconductor system, and present a detailed and realistic simulation of the pure dephasing accompanying electron tunneling in typical double QD (DQD) systems. We focus on the the controllability of the degree of this dephasing based on its understanding as a *which way* decoherence. As such, it depends on the spectral overlap of phonon wave packets, which is determined by tunneling times and g -factor mismatch only. We derive this relationship explicitly from the Weisskopf-Wigner spontaneous emission theory and make a quantitative connection between distinguishability of emitted phonons and the amount of information about spin state leaking to the environment during tunneling. By comparing these analytical calculations with the results of our dynamical simulation containing all phonon-driven and spin-orbit effects, we determine the *which way* channel to be the only relevant phonon-related spin dephasing mechanism present in the system on the relevant time scales. Qualitative understanding and quantitative characterization of this process allows us to propose ways of controlling and reducing the magnitude of dephasing via appropriate sample design and

TABLE I: Characteristics of the selected subset of modeled DQD structures used in the paper: name, QD1 radius and maximal In content, calculated g -factor mismatch between QDs, and tunneling times for electron in the two spin eigenstates at $T = 0$ K, respectively.

Structure	r_1 (nm)	c_1	Δg (10^{-3})	τ_+ (ns)	τ_- (ns)
S1	12.5	0.5	94.7	1.601	1.778
S11	12.5	0.45	36.1	0.788	0.782
S22	13.4	0.4	5.38	0.806	0.807
S25	16.1	0.4	52.8	0.223	0.221
SX	12.5	0.4112	0.00967	2.037	2.035

external fields, the latter yielding a feasible method of a real-time control over the coherence loss in real systems. The importance of our result is twofold: For the particular semiconductor system under study, the *which way* dephasing process presents a fundamental limitation to coherent spin initialization via exciton dissociation. On the other hand, the dephasing mechanism itself is generic and will affect spin coherence in transitions between states with different Zeeman splittings in any atomic, molecular or solid-state system.

We consider two vertically stacked, axially symmetric, coaxial $\text{In}_x\text{Ga}_{1-x}\text{As}$ dome-shaped QDs with a trumpet-shaped gradient of the intradot material composition [22, 23] (varying from $x = c_{1(2)}$ at QD1(2) top, down to $0.6c_{1(2)}$ at the bottom and $0.5c_{1(2)}$ in the wetting layer), in-plane base radii $r_{1(2)}$ and a fixed height/radius ratio of 1/3, separated by the distance $D = 15.6$ nm along the z axis (see Fig. 1(a)). In all calculations, parameters of QD2 are fixed at $r_2 = 12$ nm and $c_2 = 0.43$, while for QD1 are varied between $r_1 = 12.5$ – 16.1 nm and $c_1 = 0.4$ – 0.5 , which in turn alters the electron g -factor, and hence g -factor mismatch, Δg , between QDs, as well as the rates of phonon-assisted tunneling. A total of 26 structures was modeled and used in our calculations to cover the considered r_1c_1 plane with a regular grid (see Supplemental Material [24] for details). In Table I we present both structural and calculated parameters of a selected subset of structures, chosen to represent various regimes of behavior, which will serve as exemplary throughout the paper.

Electron wave functions are calculated within the 8-band $\mathbf{k} \cdot \mathbf{p}$ theory in the envelope function approximation [28–30] with spin-orbit effects, external electric and magnetic fields [31], as well as strain [32, 33] and induced piezoelectric field [34–36] up to the second order in polarization included (see Ref. [37] for details of the model and numerical methods, as well as material parameters used, except piezoelectric coefficients that are taken after [36]). An example of the electron density in the ground state is presented against the material composition profile in Fig. 1(b). As marked, the magnetic field has in-plane orientation in order to simulate magneto-

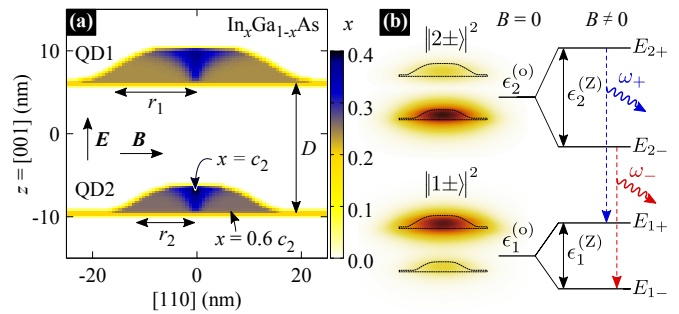


FIG. 1: (Color online) (a) A cross-section of a DQD structure (S25) material composition (yellow-blue); (b) projection of electron density (yellow-red) and a schematic diagram of energy levels; tunneling transitions are marked with blue and red dashed arrows.

optical experiments like time-resolved Faraday/Kerr rotation [38]. Additionally, we use an electric field applied along the growth axis as a fine-tuning parameter to assure that mixing of states localized in the QDs (delocalization in the ground state) is uniform among the whole ensemble of modeled DQD structures obtained by variation of QD2 parameters, i.e. in each of modeled artificial molecules the amount of electron occupation transferred during tunneling is the same. Within this model, we calculate four lowest electron states and use them as a basis set for further calculations, $\{|1+\rangle, |1-\rangle, |2+\rangle, |2-\rangle\}$ with energies $E_{1(2)\pm}$ (see Fig. 1(b) for the energy diagram), where \pm distinguishes Zeeman states and the numbers correspond to the QD in which the most of the electron density is localized. Henceforth, we shall call it for simplicity an electron in QD i with a given spin orientation, being aware of an implicit multi-band nature of these states and the partial electron delocalization essential for tunneling. For the presentation of results the $|\uparrow/\downarrow\rangle$ spin basis with respect to the z axis will also be used.

The acoustic phonon reservoir is described by $H_{\text{ph}} = \sum_{\mathbf{q}, \lambda} \hbar \omega_{\mathbf{q}, \lambda} b_{\mathbf{q}, \lambda}^\dagger b_{\mathbf{q}, \lambda}$, with $b_{\mathbf{q}, \lambda}^\dagger$ creating a λ -branch phonon with wave vector \mathbf{q} . Coupling between phonons and carriers is included via $H_{\text{int}} = H_{\text{int}}^{\text{DP}} + H_{\text{int}}^{\text{PE}}$, where the two terms account for the deformation potential and piezoelectric couplings, respectively. In the basis of $\mathbf{k} \cdot \mathbf{p}$ eigenstates, $H_{\text{int}}^{\text{DP}} = \sum_{i,j} \sigma_{ij} \int d^3\mathbf{r} \psi_i^\dagger H_{\text{BP}}^{(\text{ph})} \psi_j$, where $\sigma_{ij} = |i\rangle\langle j|$, $H_{\text{BP}}^{(\text{ph})}$ stands for the standard Bir-Pikus Hamiltonian with a phonon-induced strain-field $\hat{\epsilon}_{\text{ph}}$ [39, 40], and ψ_i is an 8-component pseudo-spinor of electron envelope functions for the i -th eigenstate spanned in the standard 8-band $\mathbf{k} \cdot \mathbf{p}$ basis. The second term accounts for the interaction of carriers with a longitudinal piezoelectric field produced by phonons and takes the form $H_{\text{int}}^{\text{PE}} = \sum_{i,j} \sigma_{ij} \int d^3\mathbf{r} \psi_i^\dagger \hat{V}_{\text{PE}}(\mathbf{r}) \psi_j$ [12], where $V_{\text{PE}}(\mathbf{r}) = i(\hat{d}\hat{\epsilon}_{\text{ph}})_{\parallel} / (\epsilon_0\epsilon_r)$, \hat{I} is the 8×8 identity, and \hat{d} is the piezoelectric tensor matrix.

Both orbital and spin degrees of freedom of electron in

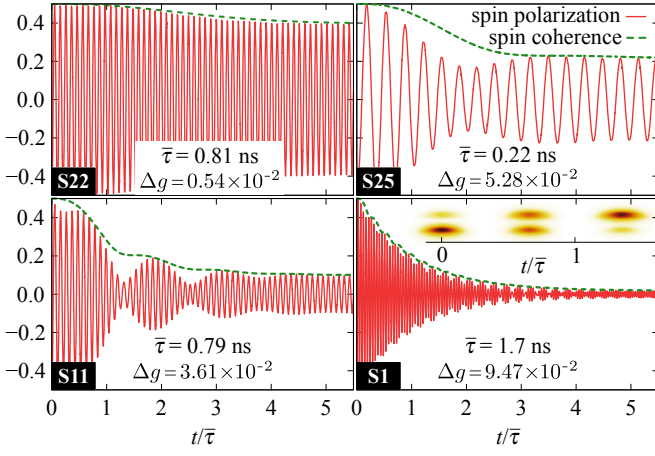


FIG. 2: (Color online) Evolution of the total spin polarization (red solid lines) and spin coherence (green dashed lines) for selected structures (number given in the bottom-left corner) in the $|\uparrow/\downarrow\rangle$ basis; the time unit is the average tunneling time, different for each structure. Inset in the bottom-right panel presents the electron density during tunneling.

the system undergo dissipative temporal evolution, which is modeled via a non-secular Markovian master equation in the Redfield form [41],

$$\dot{\rho}_e(t) = -\frac{i}{\hbar} [H_Z, \rho_e] + \pi \sum_{i,j,k,l} e^{i(\tilde{\omega}_{ij} - \tilde{\omega}_{kl})t} R_{jikl}(\omega_{kl}) \left(\sigma_{kl} \rho_e \sigma_{ij}^\dagger - \sigma_{ij}^\dagger \sigma_{kl} \rho_e \right), \quad (1)$$

written in the interaction picture with respect to $H_o = \sum_{i=1}^2 \epsilon_i^{(o)} (|i+\rangle\langle i+| + |i-\rangle\langle i-|)$, but with the Zeeman term, $H_Z = \sum_{i=1}^2 g_i \mu_B B (|i+\rangle\langle i+| - |i-\rangle\langle i-|)/2$, kept in the Schrödinger picture; here $\rho_e = \text{Tr}_{\text{ph}} \rho$ is the electron reduced density matrix, $g_i \equiv \epsilon_i^{(Z)}/(\mu_B B)$ are effective g -factors, $\epsilon_i^{(o)} = (E_{i+} + E_{i-})/2$ and $\epsilon_i^{(Z)} = E_{i+} - E_{i-}$ are energies decomposed into orbital and Zeeman contributions, $\omega_{ij} = (E_j - E_i)/\hbar$, $\tilde{\omega}_{ij} = (\epsilon_j^{(o)} - \epsilon_i^{(o)})/\hbar$, $R_{ijkl}(\omega) = \hbar^{-2} |n(\omega) + 1| \sum_{\mathbf{q},\lambda} H_{\text{int}}^{(ij)} H_{\text{int}}^{(kl)} \delta(|\omega| - \omega_{\mathbf{q},\lambda})$ are phonon spectral densities describing the phonon-driven dissipative dynamics [12], $H_{\text{int}}^{(ij)} = \langle i|H_{\text{int}}|j\rangle$, $n(\omega)$ is the Bose distribution and $\omega_{\mathbf{q},\lambda}$ are phonon frequencies. Tunneling times for electrons in the two spin states are determined from the Fermi golden rule, $\tau_{\pm} = [2\pi R_{ijji}(\omega_{ji})]^{-1}$ with $i = 2\pm$, $j = 1\pm$. A numerical solution of Eq. (1) provides us with complete information about the evolution of the system, via the diagonal (occupations) and off-diagonal (coherences) matrix elements of ρ_e . Throughout the paper, the initial state will be set to $|2\uparrow\rangle = (|2+\rangle + |2-\rangle)/\sqrt{2}$, which corresponds to an optical initialization with an appropriate circular polarization in the experiment. Unless otherwise stated, the calculations are done for $B = 5$ T and $T = 0$ K.

We begin the discussion of results with an overview of

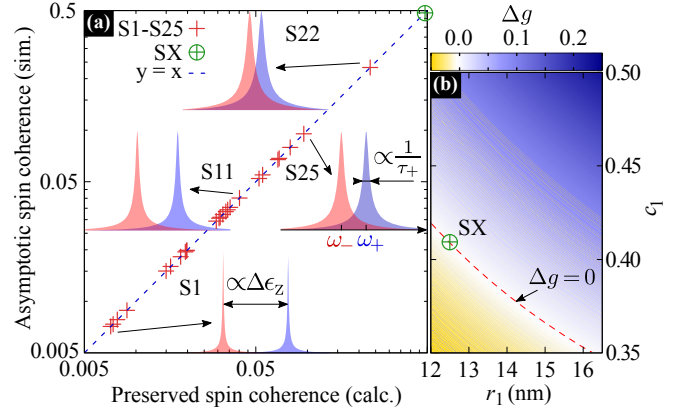


FIG. 3: (Color online) (a) Asymptotic spin coherence from simulation via Eq. (1) vs. preserved coherence calculated according to the Weisskopf-Wigner theory, Eq. (2), for structures S1-S25 (red crosses) and SX (green cross in a circle) designed to reduce decoherence; the value of 0.5 means a pure state; the insets present spectral overlaps of phonon wave packets emitted during tunneling of two opposite spins for selected structures. (b) Dependence of the g -factor mismatch on QD1 size and In content extrapolated from data obtained for simulated structures; dashed red line marks $\Delta g = 0$.

spin dynamics during electron tunneling in the magnetic field, presented in Fig. 2, where the evolution of the total spin polarization and spin coherence is plotted for selected DQD structures differing mainly in the mismatch of Zeeman splittings between QDs, $\Delta\epsilon_Z = \Delta g \mu_B B$ (see Table I). One may notice damping of spin precession accompanied by a proportional spin coherence loss, both related to but not uniquely determined by the Zeeman splitting mismatch, which suggests there is another factor involved. Note that decoherence takes place once in the course of tunneling, as the spin coherence becomes nearly constant after a few tunneling times interval in each of the cases. Beating in spin polarization during tunneling is due to the difference in precession frequencies between QDs.

To quantitatively associate this decoherence with the *which way* process we calculate spin coherence after tunneling within the Weisskopf-Wigner [42, 43] theory of spontaneous emission adapted to the phonon bath (see Supplemental Material [24]). This gives the amount of coherence that would be preserved after tunneling if the only dephasing in the system originated from the spontaneous emission of nonidentical phonons, which is exactly the process under consideration. In this approach, the preserved coherence may be calculated as an overlap of reservoir states produced during tunneling of opposite spins, $C = \langle R_+ | R_- \rangle$, where $|R_{\pm}\rangle \propto \sum_{\mathbf{q},\lambda} c_{\mathbf{q},\lambda}^{(\pm)} \sigma_{\mathbf{q},\lambda}^\dagger |R_0\rangle$, $|R_0\rangle$ is the initial state of the bath, and $c_{\mathbf{q},\lambda}^{(\pm)} \propto [(\omega_{\mathbf{q},\lambda} - \tilde{\omega}_{12} \pm \Delta\epsilon_Z/\hbar) + i/(2\tau_{\pm})]^{-1}$ describe the distribution of phonon modes in emitted wave pack-

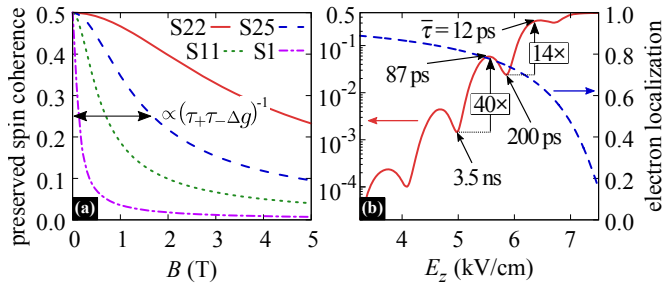


FIG. 4: (Color online) (a) Dependence of preserved spin coherence on magnetic field for selected structures. (b) Dependence of preserved spin coherence (red solid line, left axis) and electron localization (blue dashed line, right axis) on external electric field oriented along the z -axis for structure S11; possible changes in coherence value are marked with vertical arrows, tunneling times are given at extrema.

ets (see insets in Fig. 3(a)). The derivation [24] yields

$$C \simeq \frac{1}{\sqrt{\tau_+ \tau_- \left[\left(\frac{2\Delta\epsilon_z}{\hbar} \right)^2 + \left(\frac{1}{\tau_+} + \frac{1}{\tau_-} \right)^2 \right]}}, \quad (2)$$

which is defined by the Zeeman splitting mismatch and tunneling times only. Although shorter tunneling times are favorable for higher coherence it is not a matter of competition between the tunneling rate and some kind of decoherence rate. In fact, the dephasing is a one-time process tied to the tunneling and is not characterized by a rate; instead, the characteristic parameter is the mismatch of Zeeman splittings which is not related to any rate.

In Fig. 3(a) we confront the preserved spin coherence calculated according to Eq. (2) with its asymptotic values from our dynamical simulation for a set of 25 structures and find these two to coincide perfectly, which confirms our assumption on the dominant decoherence mechanism and, additionally, shows it to be the only relevant spin dephasing channel present in the system. Moreover, one may notice that with the variation of QD1 size and composition within reasonable ranges it is possible to cover a full range of preserved coherence values. We propose to use this tunability to design structures of desired properties. The green circle shows the result obtained for an additional structure, SX, intentionally designed to switch off spin dephasing by reducing Δg by fine-tuning structure parameters, based on the extrapolated dependence of Δg on r_1 and c_1 (see Supplemental Material [24]) presented as a color map in Fig. 3(b).

Controlling the degree of dephasing by tuning the g -factor mismatch at the stage of QD growth obviously requires extremely precise manufacturing technology and may not be feasible. A practical control protocol should rely on external fields applied to the sample. Obviously, since dephasing is due to the mismatch of Zeeman split-

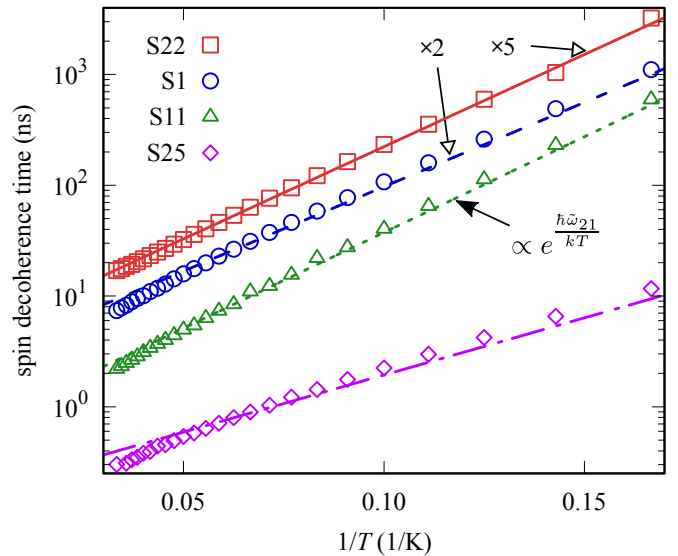


FIG. 5: (Color online) Dependence of spin decoherence times on temperature for selected structures (open symbols) and theoretical curves for activation process with respective tunneling transition energies (lines). Results for S1 and S22 are shifted for visibility.

tings, it can be eliminated by reducing the magnitude of the magnetic field. The magnetic field dependence of the preserved coherence is plotted in Fig. 4(a) for selected structures. The dependence is Lorentzian-like with a width proportional to $1/(\tau_+ \tau_- \Delta g)$. Thus, on the one hand, tuning the system into a fast tunneling regime (structure S22, solid red line) may be used to widen the range of magnetic fields for which tunneling is reasonably coherent. On the other hand, slow tunneling allows one to switch between coherent and incoherent tunneling with small changes in low magnetic field, e.g. coherence changes between 0.035 and 0.5 for B under 1 T in the case of S1 (dash-dotted magenta line).

Another feasible way of controlling spin decoherence in the system is to take advantage of the oscillation of tunneling rates versus transition energy (with a period connected to the inter-dot distance) [44, 45]. The latter may be tuned with an axial electric field. However, this changes the state mixing between QDs (degree of electron localization, up to now was kept on a fixed level). Both these dependencies are plotted in Fig. 4(b). We find that decoherence can be controlled within a range of values extending over many orders of magnitude, while still keeping the electron localized and within reasonable tunneling times regime.

Saturation of spin coherence in Fig. 2 results from the fact that tunneling at $T = 0$ is irreversible, hence the decoherence process takes place only once. In contrast, at $T > 0$ thermally activated back-tunneling becomes possible, which turns the spin dephasing into a continuous process, accompanying the repeated virtual tunneling be-

tween the dots. Both analytical results from the Master equation and numerical simulations predict a simple exponential decay in this case as discussed in detail in the Supplemental Material [24]. The dependence of the coherence decay time on temperature is shown in Fig. 5. Each simulation result can be fitted by an exponential function representing a thermally activated process with an appropriate transition energy (lines in Fig. 5).

In summary, we have presented a theoretical prediction of a spin dephasing channel for a spin-preserving tunneling of electrons between two coupled subsystems in a magnetic field. The dephasing originates from distinguishability of reservoir excitations induced by dissipative tunneling in the two opposite spin states, and hence the resulting leakage of information about the spin state to the environment. The process in question is thus of fundamental nature and analogous to those resulting from measuring the particle position in double-slit experiments. While the dephasing mechanism is general, we have presented its detailed quantitative analysis for coupled self-assembled QDs, based on realistic multi-band $\mathbf{k} \cdot \mathbf{p}$ modeling and dynamical simulations of orbital and spin degrees of freedom using a non-secular Markovian master equation, combined with an analysis of reservoir state indistinguishability. The effect has been shown to essentially depend on the mismatch in electron g -factors in the two dots and also scale with tunneling times, both of which define the spectral overlap of emitted phonon wave packets corresponding to the two spin orientations. Additionally, we have proved that the predicted effect is the only phonon-related dephasing mechanism relevant in the discussed system. Finally, we have proposed ways of controlling spin decoherence both at the manufacturing stage via size and composition of coupled QDs, as well as on demand, by appropriate tuning of external fields. The latter promises a feasible method of a real-time control over spin decoherence across many orders of magnitude.

K. G. and P. M. acknowledge support by the Grant No. 2014/12/B/ST3/04603 from the Polish National Science Centre (Narodowe Centrum Nauki). M. G. acknowledges support by the Grant No. 2011/02/A/ST3/00152 from the Polish National Science Centre, and would like to thank M. Syperek for an inspiring discussion. Part of calculations has been carried out using resources provided by Wrocław Centre for Networking and Supercomputing (<http://wcss.pl>), grant No. 203.

* Electronic address: michal.gawelczyk@pwr.edu.pl

- [1] R. P. Feynman, *Int. J. Theor. Phys.* **21**, 467 (1982).
 [2] R. P. Feynman, R. B. Leighton, and M. Sands, *The Feynman Lectures on Physics, Vol. I: The New Millennium Edition: Mainly Mechanics, Radiation, and Heat* (Basic Books, 2010).
 [3] P. Sonnentag and F. Hasselbach, *Phys. Rev. Lett.* **98**,

- 200402 (2007).
 [4] E. Joos, H. D. Zeh, C. Kiefer, D. J. W. Giulini, J. Kupsch, and I.-O. Stamatescu, *Decoherence and the Appearance of a Classical World in Quantum Theory* (Springer, 2003).
 [5] M. A. Schlosshauer, *Decoherence and the Quantum-To-Classical Transition* (Springer, 2007).
 [6] A. Galindo and M. A. Martín-Delgado, *Rev. Mod. Phys.* **74**, 347 (2002).
 [7] N. Gisin, G. Ribordy, W. Tittel, and H. Zbinden, *Rev. Mod. Phys.* **74**, 145 (2002).
 [8] T. Korn, *Phys. Rep.* **494**, 415 (2010).
 [9] I. Žutić, J. Fabian, and S. Das Sarma, *Rev. Mod. Phys.* **76**, 323 (2004).
 [10] D. Awschalom, D. Loss, and N. Samarth, *Semiconductor spintronics and quantum computation* (Springer, 2002).
 [11] R. Hanson, L. P. Kouwenhoven, J. R. Petta, S. Tarucha, and L. M. K. Vandersypen, *Rev. Mod. Phys.* **79**, 1217 (2007).
 [12] K. Roszak, A. Grodecka, P. Machnikowski, and T. Kuhn, *Phys. Rev. B* **71**, 195333 (2005).
 [13] A. Grodecka, P. Machnikowski, and J. Förstner, *Phys. Rev. A* **79**, 042331 (2009).
 [14] A. J. Ramsay, S. J. Boyle, R. S. Kolodka, J. B. B. Oliveira, J. Skiba-Szymanska, H. Y. Liu, M. Hopkinson, A. M. Fox, and M. S. Skolnick, *Phys. Rev. Lett.* **100**, 197401 (2008).
 [15] T. M. Godden, S. J. Boyle, A. J. Ramsay, A. M. Fox, and M. S. Skolnick, *Appl. Phys. Lett.* **97**, 061113 (2010).
 [16] K. Müller, A. Bechtold, C. Ruppert, C. Hautmann, J. S. Wildmann, T. Kaldewey, M. Bichler, H. J. Krenner, G. Abstreiter, M. Betz, and J. J. Finley, *Phys. Rev. B* **85**, 241306 (2012).
 [17] T. M. Godden, J. H. Quilter, A. J. Ramsay, Y. Wu, P. Brereton, I. J. Luxmoore, J. Puebla, A. M. Fox, and M. S. Skolnick, *Phys. Rev. B* **85**, 155310 (2012).
 [18] T. M. Godden, J. H. Quilter, A. J. Ramsay, Y. Wu, P. Brereton, S. J. Boyle, I. J. Luxmoore, J. Puebla-Nunez, A. M. Fox, and M. S. Skolnick, *Phys. Rev. Lett.* **108**, 017402 (2012).
 [19] M. Krzykowski, M. Gawelczyk, and P. Machnikowski, *Acta Phys. Pol. A* **130**, 1165 (2016).
 [20] M. Kroutvar, Y. Ducommun, D. Heiss, M. Bichler, D. Schuh, G. Abstreiter, and J. J. Finley, *Nature* **432**, 81 (2004).
 [21] M. Kugler, K. Korzekwa, P. Machnikowski, C. Gradl, S. Furthmeier, M. Griesbeck, M. Hirmer, D. Schuh, W. Wegscheider, T. Kuhn, C. Schüller, and T. Korn, *Phys. Rev. B* **84**, 085327 (2011).
 [22] M. A. Migliorato, A. G. Cullis, M. Fearn, and J. H. Jefferson, *Phys. Rev. B* **65**, 115316 (2002).
 [23] V. Jovanov, T. Eissfeller, S. Kapfinger, E. C. Clark, F. Klotz, M. Bichler, J. G. Keizer, P. M. Koenraad, M. S. Brandt, G. Abstreiter, and J. J. Finley, *Phys. Rev. B* **85**, 165433 (2012).
 [24] See Supplemental Material for details of the ensemble of modeled structures, derivation of preserved coherence within general theory based on distinguishability of environment states, description of extrapolation of g -factor mismatch dependence on size and composition of QD1, as well as analytical analysis of dephasing at finite temperature.
 [25] T. Nakaoka, T. Saito, J. Tatebayashi, and Y. Arakawa, *Phys. Rev. B* **70**, 235337 (2004).
 [26] J. van Bree, A. Y. Silov, P. M. Koenraad, M. E. Flatté,

- and C. E. Pryor, Phys. Rev. B **85**, 165323 (2012).
- [27] I. Vurgaftman, J. R. Meyer, and L. R. Ram-Mohan, Journal of Applied Physics **89**, 5815 (2001).
- [28] M. G. Burt, J. Phys. Condens. Matter **4**, 6651 (1992).
- [29] B. A. Foreman, Phys. Rev. B **48**, 4964 (1993).
- [30] T. B. Bahder, Phys. Rev. B **41**, 11992 (1990).
- [31] T. Andlauer, R. Morschl, and P. Vogl, Phys. Rev. B **78**, 075317 (2008).
- [32] G. Bir and G. Pikus, *Symmetry and Strain-induced Effects in Semiconductors*, A Halsted Press book (Wiley, 1974).
- [33] C. Pryor, Phys. Rev. B **57**, 7190 (1998).
- [34] G. Bester, X. Wu, D. Vanderbilt, and A. Zunger, Phys. Rev. Lett. **96**, 187602 (2006).
- [35] S. Schulz, M. A. Caro, E. P. O'Reilly, and O. Marquardt, Phys. Rev. B **84**, 125312 (2011).
- [36] G. Tse, J. Pal, U. Monteverde, R. Garg, V. Haxha, M. A. Migliorato, and S. Tomić, J. Appl. Phys. **114**, 073515 (2013).
- [37] K. Gawarecki, P. Machnikowski, and T. Kuhn, Phys. Rev. B **90**, 085437 (2014).
- [38] J. J. Baumberg, D. D. Awschalom, N. Samarth, H. Luo, and J. K. Furdyna, Phys. Rev. Lett. **72**, 717 (1994).
- [39] L. M. Woods, T. L. Reinecke, and R. Kotlyar, Phys. Rev. B **69**, 125330 (2004).
- [40] K. Roszak, V. M. Axt, T. Kuhn, and P. Machnikowski, Phys. Rev. B **76**, 195324 (2007).
- [41] F. Breuer, H. and Petruccione, *The Theory of Open Quantum Systems* (Oxford University Press, 2007).
- [42] V. Weisskopf and E. Wigner, Zeitschrift für Physik **63**, 54 (1930).
- [43] M. O. Scully and M. S. Zubairy, *Quantum Optics* (Cambridge University Press, 1997).
- [44] K. C. Wijesundara, J. E. Rolon, S. E. Ulloa, A. S. Bracker, D. Gammon, and E. A. Stinaff, Phys. Rev. B **84**, 081404 (2011).
- [45] K. Gawarecki, M. Pochwała, A. Grodecka-Grad, and P. Machnikowski, Phys. Rev. B **81**, 245312 (2010).

Supplemental material: Controllable electron spin dephasing due to phonon state distinguishability in a coupled quantum dot system

Michał Gawelczyk,^{1,2} Mateusz Krzykowski,² Krzysztof Gawarecki,² and Paweł Machnikowski²

¹*Department of Experimental Physics, Faculty of Fundamental Problems of Technology, Wrocław University of Science and Technology, Wybrzeże Stanisława Wyspiańskiego 27, 50-370 Wrocław, Poland*

²*Department of Theoretical Physics, Faculty of Fundamental Problems of Technology, Wrocław University of Science and Technology, Wybrzeże Stanisława Wyspiańskiego 27, 50-370 Wrocław, Poland*

This supplemental material is organized in the following way. In Sec. AI we define the ensemble of modeled DQD structures used in the paper. Next, in Sec. AII we describe the method used to extrapolate numerically calculated values of g -factor mismatch and obtain an approximate formula for its continuous dependence on size and composition of QD1. In Sec. AIII we derive the expression for preserved spin coherence (Eq. (2) in the paper) within a general theory of spontaneous emission. Finally, in Sec. AIV we give a detailed description of the spin decoherence at finite temperatures. Numbers of all sections, figures, tables and equations within this document are preceded by the capital letter A, while all the other apply to the content of the main paper.

AI. MODELED STRUCTURES

The details of the ensemble of DQD structures used in simulations are as follows. A total of 27 numerically modeled structures were used in our calculations. Those labeled by S1-S25 differ in the QD1 base radius r_1 and indium composition c_1 , and form a 5×5 grid in the (r_1, c_1) parameter plane, regular with respect to each of the axes. Additional two structures, labeled SX and SY, were used to simulate dephasing-free systems and will be discussed in the next section. Characteristics of all the structures are presented in Table AI, where also calculated g -factor mismatch, tunneling times and transition energies as well as preserved spin coherence values are given. Additionally, in Fig. A1 the structures are represented in the (r_1, c_1) plane.

AII. EXTRAPOLATION OF RESULTS

In this section we present details of the extrapolation procedure that has been used to obtain the dependence of g -factor mismatch on the size and composition of QD1, which is presented as a color map in Fig. 3(b). We use g -factor mismatch values, Δg , calculated for all structures in the ensemble (S1-S25) to probe the $r_1 c_1$ plane and obtain an extrapolated dependence, $\Delta g = f(r_1, c_1)$. Expecting a close to linear dependence of electron g -factor on a uniform size change of the QD^{1,2} and terms up to quadratic in the dependence on In concentration (inherited after quadratic corrections to the interpolation of the bulk g -factor between GaAs and InAs, commonly referred to as bowing³) we use

$$\Delta g(r_1, c_1) \approx \sum_{n=0}^1 \sum_{m=0}^2 c_{nm} r_1^n c_1^m \quad (\text{A1})$$

and obtain the set of c_{nm} coefficients by fitting this function to Δg values obtained numerically for simulated structures, using the least squares method (see Table AII for obtained coefficients). The resulting depen-

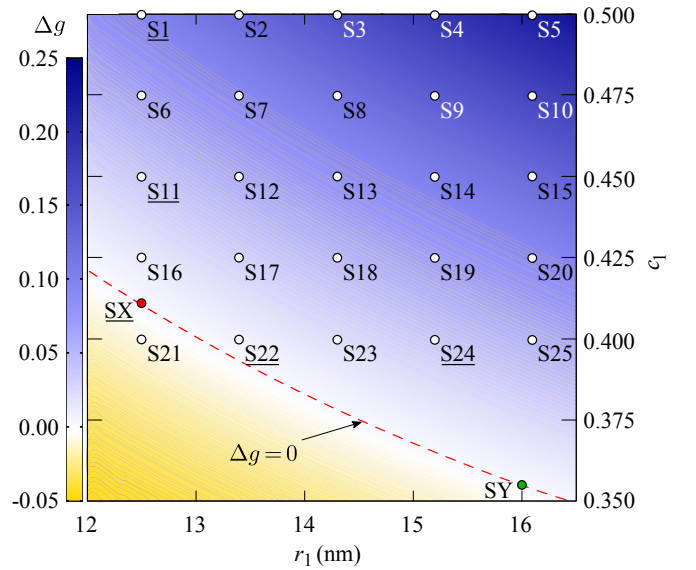


FIG. A1: (Color online) Dependence of the g -factor mismatch on QD1 size (r_1) and In content (c_1) extrapolated from data obtained for simulated structures S1-S25 via fitting of Eq. (A1) to numerically calculated values; the dashed red line marks $\Delta g = 0$. Parameters of structures are represented by positions of dots with their labels (underlined in case of those used as exemplary in the paper) at respective points of the map.

dence, $\Delta g(r_1, c_1)$, is presented in Fig. A1 as a color map together with an estimated line of $\Delta g = 0$. Following the latter, SX was designed to diminish the g -factor mismatch via tuning of In content of S21 (see Table AI for characteristics of structures). To check the range of applicability of the fit, another structure, labeled SY, was designed with the value of c_1 aiming in the predicted $\Delta g = 0$ line, but far from the area of parameters covered by the ensemble of structures taken for the fitting procedure. The numerically calculated value of $\Delta g \sim 10^{-4}$ in this case proves the fit is sufficiently good for its purpose in the considered range of parameters.

TABLE AI: Characteristics of all the modeled DQD structures used in the paper: name, QD1 radius and maximal In content, calculated g -factor mismatch between states localized in the two QDs, tunneling times at $T = 0$ K and transition energies for the two spin states, as well as preserved spin coherence, respectively. Structures used as exemplary in the paper are highlighted.

	r_1 (nm)	c_1	Δg (10^{-3})	τ_+ (ns)	τ_- (ns)	$\hbar\omega_+$ (meV)	$\hbar\omega_-$ (meV)	$ C $ 10^{-3}
S1	12.5	0.5	94.7	1.60	1.78	3.02	2.99	7.14
S2	13.4	0.5	123	0.636	0.527	2.52	2.49	16.0
S3	14.3	0.5	153	0.237	0.226	2.13	2.08	32.2
S4	15.2	0.5	183	0.301	0.329	1.81	1.75	19.9
S5	16.1	0.5	213	0.607	0.601	1.52	1.46	8.86
S6	12.5	0.475	63.7	0.892	0.921	3.21	3.20	19.7
S7	13.4	0.475	88.6	1.80	1.51	2.71	2.67	7.82
S8	14.3	0.475	114	0.294	0.269	2.28	2.24	35.4
S9	15.2	0.475	140	0.241	0.243	1.96	1.92	33.4
S10	16.1	0.475	167	0.431	0.483	1.65	1.61	15.0
S11	12.5	0.45	36.0	0.788	0.782	3.43	3.42	40.2
S12	13.4	0.45	57.2	2.65	2.77	2.88	2.86	7.36
S13	14.3	0.45	79.2	0.496	0.445	2.44	2.41	30.6
S14	15.2	0.45	101	0.214	0.214	1.99	1.96	52.2
S15	16.1	0.45	125	0.302	0.320	1.77	1.74	29.4
S16	12.5	0.425	11.8	1.21	1.19	3.66	3.66	79.4
S17	13.4	0.425	29.4	1.23	1.26	3.06	3.05	31.0
S18	14.3	0.425	48.0	1.28	1.16	2.61	2.59	19.4
S19	15.2	0.425	67.1	0.256	0.245	2.20	2.18	67.3
S20	16.1	0.425	86.8	0.236	0.239	1.90	1.88	54.8
S21	12.5	0.4	-8.83	3.72	3.79	3.91	3.90	34.3
S22	13.4	0.4	5.38	0.806	0.807	3.30	3.30	233
S23	14.3	0.4	20.5	3.04	3.05	2.80	2.79	18.2
S24	15.2	0.4	36.3	0.467	0.444	2.39	2.38	68.3
S25	16.1	0.4	52.8	0.223	0.221	2.05	2.03	95.2
SX	12.5	0.4112	0.00967	2.04	2.04	3.72	3.72	499
SY	16.0	0.353	0.354	-	-	-	-	-

TABLE AII: Coefficients obtained from fitting function (A1) to numerically calculated Δg values.

m \ n	0	1	2
0	0.42096	-0.023023	1.3877
1	-2.1669	0.055439	0.11238

AIII. DECOHERENCE DUE TO DISTINGUISHABILITY OF ENVIRONMENT STATES

The process of spin-preserving tunneling may be asymptotically described as

$$(C_+ |2+\rangle + C_- |2-\rangle) \otimes |R_0\rangle \rightarrow (C_+ |1+\rangle \otimes |R_+\rangle + C_- |1-\rangle \otimes |R_-\rangle),$$

where coefficients C_\pm define the spin superposition, $|R_0\rangle$ is the phonon bath initial state, and the bath states produced during tunneling of electron with two spin orientations may be expanded in the basis of phonon modes as

$$|R_\pm\rangle = \sum_{\mathbf{q},\lambda} \frac{c_{\mathbf{q},\lambda}^{(\pm)}}{\sqrt{n_{\mathbf{q},\lambda} + 1}} b_{\mathbf{q},\lambda}^\dagger |R_0\rangle,$$

where $c_{\mathbf{q},\lambda}^{(\pm)}$ are complex coefficients. The relevant part of the reduced density matrix (for the target dot, i.e. QD1 spatial subspace) after tunneling is thus

$$\rho_e^{(\text{QD1})}(\infty) = \begin{pmatrix} |C_-|^2 & C_-^* C_+ \langle R_- | R_+ \rangle \\ C_+^* C_- \langle R_+ | R_- \rangle & |C_+|^2 \end{pmatrix},$$

and spin coherence preserved in the process may be found from its off-diagonal element as

$$\begin{aligned} C &= \langle 1- | \rho_e | 1+ \rangle = C_-^* C_+ \langle R_- | R_+ \rangle \\ &= C_-^* C_+ \sum_{\mathbf{q},\lambda} \sum_{\mathbf{q}',\lambda'} \frac{c_{\mathbf{q},\lambda}^{(-)*}}{\sqrt{n_{\mathbf{q},\lambda} + 1}} \frac{c_{\mathbf{q}',\lambda'}^{(+)}}{\sqrt{n_{\mathbf{q}',\lambda'} + 1}} \langle b_{\mathbf{q},\lambda} b_{\mathbf{q}',\lambda'}^\dagger \rangle_{R_0} \\ &= C_-^* C_+ \sum_{\mathbf{q},\lambda} c_{\mathbf{q},\lambda}^{(-)*} c_{\mathbf{q},\lambda}^{(+)}. \end{aligned} \quad (\text{A2})$$

The phonon reservoir states (defined by the sets of $c_{\mathbf{q},\lambda}^{(\pm)}$) may be calculated within the Wigner-Weisskopf theory of spontaneous emission from a two-level system^{4,5}, adapted here to the case of phonon reservoir and distinct tunneling channels for the two spin states. We begin with a Hamiltonian describing the coupling of the carrier subsystem to phonon modes written in the interaction picture and rotating-wave approximations⁶

$$\tilde{H}_{\text{e-ph}}^{\text{RWA}} = \hbar \sum_{\eta=\pm} \sigma_{12}^{(\eta)} \sum_{\mathbf{q},\lambda} g_{\mathbf{q},\lambda}^{(\eta)*} b_{\mathbf{q},\lambda} e^{i(\omega_\eta - \omega_{\mathbf{q},\lambda})t} + \text{H.c.},$$

where $\sigma_{12}^{(\eta)} = |1\eta\rangle\langle 2\eta|$, $\omega_\pm = \tilde{\omega}_{12} \pm \Delta\epsilon_Z/2\hbar$ are the tunneling transition frequencies, $g_{\mathbf{q},\lambda}^{(\pm)} = \langle 1 \pm | H_{\text{int}}^{(\mathbf{q},\lambda)} | 2\pm \rangle / \hbar$ is the electron-phonon coupling constant; $g_{\mathbf{q},\lambda}^{(+)} = g_{\mathbf{q},\lambda}^{(-)*} \equiv g_{\mathbf{q},\lambda}$, $\omega_{\mathbf{q},\lambda} = qc_\lambda$, and c_λ is the speed of sound. We look for a solution describing the spin-preserving tunneling by imposing the time dependence of $c_{\mathbf{q},\lambda}^{(\pm)}$, i.e.

$$\begin{aligned} |\psi(t)\rangle &= c_2(t) \left(C_+ |2+\rangle + C_- |2-\rangle \right) \otimes |R_0\rangle \\ &+ \sum_{\eta=\pm} \sum_{\mathbf{q},\lambda} C_\eta |1\eta\rangle \otimes \left(\frac{c_{\mathbf{q},\lambda}^{(\eta)}(t) b_{\mathbf{q},\lambda}^\dagger |R_0\rangle}{\sqrt{n_{\mathbf{q},\lambda} + 1}} \right). \end{aligned}$$

The Schrödinger equation, $|\dot{\psi}(t)\rangle = -(i/\hbar) \tilde{H}_{\text{e-ph}}^{\text{RWA}} |\psi(t)\rangle$, may be transformed to a linear integro-differential equation for $c_2(t)$

$$\dot{c}_2(t) = - \sum_{\eta=\pm} \sum_{\mathbf{q},\lambda} \left| g_{\mathbf{q},\lambda}^{(\eta)} \right|^2 \int_0^t dt' e^{i(\omega_\eta - \omega_{\mathbf{q},\lambda})(t-t')} c_2(t'),$$

where, after replacing the sum over the wave vector with an integral in the spherical coordinates, the leading contribution comes from the vicinity of $\omega_\eta = \omega_{\mathbf{q},\lambda}$, which leads to the solution $c_2(t) = c_2(0)e^{-\Gamma t}$, where $\Gamma = \Gamma_+ + \Gamma_-$. Here, Γ_\pm are the tunneling rates for the two spin eigenstates (consistent with those defined in the paper within the theory of open quantum systems),

$$\Gamma_\pm = 4\pi \frac{V\omega_\pm^2}{16\pi^3} \sum_\lambda \frac{1}{c_\lambda^3} \int_\Omega d\Omega \sin\theta |g_{\mathbf{q}\pm,\lambda}|^2, \quad (\text{A3})$$

where V is the unit cell volume, Ω the solid angle, and $\mathbf{q}\pm \equiv (\omega_\pm/c_\lambda, \phi, \theta)$ is a phonon wave vector with a fixed magnitude corresponding to the frequency of the emitted phonon. The solution for $c_{\mathbf{q},\lambda}^{(\pm)}(t)$ is then

$$c_{\mathbf{q},\lambda}^{(\pm)}(t) = g_{\mathbf{q},\lambda}^{(\pm)} \frac{1 - e^{i(\omega_{\mathbf{q},\lambda} - \omega_\pm)t - \frac{\Gamma_\pm}{2}t}}{(\omega_{\mathbf{q},\lambda} - \omega_\pm) + i\frac{\Gamma_\pm}{2}},$$

which, in the limit of $t \rightarrow \infty$, gives desired asymptotic coefficients

$$c_{\mathbf{q},\lambda}^{(\pm)} = \frac{g_{\mathbf{q},\lambda}^{(\pm)}}{(\omega_{\mathbf{q},\lambda} - \omega_\pm) + \frac{i}{2\tau_\pm}}.$$

Now, after replacing the sum over the wave vector with an integral in the spherical coordinates in Eq. (A2) it becomes

$$C = C_-^* C_+ \frac{V}{16\pi^3} \sum_\lambda \frac{1}{c_\lambda^3} \int_\Omega d\Omega \sin\theta \int_0^{\omega_\lambda^{(D)}} d\omega_{\mathbf{q},\lambda} \frac{\omega_{\mathbf{q},\lambda}^2 |g_{\mathbf{q},\lambda}|^2}{\left(\omega_{\mathbf{q},\lambda} - \omega_- - \frac{i}{2\tau_-}\right) \left(\omega_{\mathbf{q},\lambda} - \omega_+ + \frac{i}{2\tau_+}\right)},$$

where $\omega_\lambda^{(D)}$ is the Debye frequency. In the integrand, the denominator defines two peaks centered at ω_\pm and widened by $1/\tau_\pm$, compared to which the numerator varies slowly with $\omega_{\mathbf{q},\lambda}$. Using this fact, we substitute $(\omega_+^2 |g_{\mathbf{q}+, \lambda}|^2 + \omega_-^2 |g_{\mathbf{q}-, \lambda}|^2)/2$ for it (which would be exact in the limit of equal Dirac delta peaks). As $1/\tau_\pm \ll \omega_\pm \ll \omega_\lambda^{(D)}$, the limits of integration over frequency may be extended to $\pm\infty$ and we obtain

$$C \simeq \frac{C_-^* C_+}{2} \sum_{\eta=\pm} \left(\frac{V\omega_\eta^2}{16\pi^3} \sum_\lambda \frac{1}{c_\lambda^3} \int_\Omega d\Omega \sin\theta |g_{\mathbf{q}\eta,\lambda}|^2 \right) \times \int_{-\infty}^{\infty} \frac{d\omega}{\left[(\omega - \omega_-) - \frac{i}{2\tau_-}\right] \left[(\omega - \omega_+) + \frac{i}{2\tau_+}\right]}.$$

Comparing this with Eq. (A3) we get

$$\begin{aligned} C &\simeq \frac{C_-^* C_+ \Gamma}{4\pi} \int_{-\infty}^{\infty} \frac{d\omega}{\left[(\omega - \omega_-) - \frac{i}{2\tau_-}\right] \left[(\omega - \omega_+) + \frac{i}{2\tau_+}\right]} \\ &\simeq C_-^* C_+ \int_{-\infty}^{\infty} d\omega \frac{\sqrt{\frac{\Gamma_-}{2\pi}}}{(\omega - \omega_-) - \frac{i\Gamma_-}{2}} \frac{\sqrt{\frac{\Gamma_+}{2\pi}}}{(\omega - \omega_+) + \frac{i\Gamma_+}{2}} \\ &= C_-^* C_+ \int_{-\infty}^{\infty} d\omega \sqrt{\mathcal{L}_{\omega_-, \Gamma_-}(\omega)}^* \sqrt{\mathcal{L}_{\omega_+, \Gamma_+}(\omega)}, \end{aligned}$$

where $\mathcal{L}_{\omega, \Gamma}$ is the Lorentzian function and we have made use of the approximate equality of geometric and arithmetic means as $|\Gamma_+ - \Gamma_-| \ll \Gamma_\pm$. Finally, the evaluation of the last integral gives

$$C \simeq \frac{C_-^* C_+}{\sqrt{\tau_+ \tau_- \left[\left(\frac{2\Delta\epsilon_Z}{\hbar} \right)^2 + \left(\frac{1}{\tau_+} + \frac{1}{\tau_-} \right)^2 \right]}},$$

which for the case of the equal spin superposition with $C_\pm = 1/\sqrt{2}$ yields the Eq. (2) used in the paper.

AIV. SPIN DECOHERENCE AT FINITE TEMPERATURE

A non-zero probability of back-tunneling at finite temperature results in an additional process of continuous accumulative spin decoherence. Here, we work in the interaction picture also with respect to the Zeeman Hamiltonian, as we are not explicitly interested in spin precession. For simplicity, we neglect all spin-flip processes, namely spin relaxation within a QD and spin-flip accompanied tunneling, as these have no observable contribution to spin decoherence in the considered timescale, as has been proven in the paper via numerical simulations. This corresponds to setting $R_{ijkl} = 0$ in the Master equation, Eq. (1), if any of the two pairs of indices, (ij) or (kl) , is not matched in a spin state (\pm) . Additionally, we assume all diagonal electron-phonon couplings to be equal, which means that all R_{iikl} and R_{klli} are i -independent. Such simplification partly decouples the time evolution of density matrix elements, in particular yields a closed set of two equations for spin coherences,

$$\begin{aligned} \langle 1|\rho_e|2 \rangle &\simeq -\pi [R_{4224}(\omega_{42}) + R_{3113}(\omega_{31})] \langle 1|\rho_e|2 \rangle \\ &\quad + \pi [R_{1342}(\omega_{24}) + R_{1342}(\omega_{13})] e^{i(\omega_{24} - \omega_{13})t} \langle 3|\rho_e|4 \rangle, \\ \langle 3|\rho_e|4 \rangle &\simeq -\pi [R_{4224}(\omega_{24}) + R_{3113}(\omega_{13})] \langle 3|\rho_e|4 \rangle \\ &\quad + \pi [R_{3124}(\omega_{31}) + R_{3124}(\omega_{42})] e^{i(\omega_{13} - \omega_{24})t} \langle 1|\rho_e|2 \rangle, \end{aligned} \quad (\text{A4})$$

where we have changed state labels from $\{1-, 1+, 2-, 2+\}$ to $\{1, 2, 3, 4\}$ for clarity.

First, we check the $T = 0$ K limit. Considering that $R_{ijkl}(\omega_{mn}) = \exp(-\frac{\hbar\omega_{nm}}{kT}) R_{ijkl}(\omega_{nm})$, spectral densities with $m > n$ describe thermally activated processes and

vanish, hence the equations are simplified to

$$\begin{aligned} \langle 1|\dot{\rho}_e^{(0K)}|2\rangle &\simeq \pi [R_{1342}(\omega_{24}) + R_{1342}(\omega_{13})] \langle 3|\rho_e^{(0K)}|4\rangle \\ &\quad \times e^{i(\omega_{24}-\omega_{13})t}, \\ \langle 3|\dot{\rho}_e^{(0K)}|4\rangle &\simeq -\pi [R_{4224}(\omega_{24}) + R_{3113}(\omega_{13})] \langle 3|\rho_e^{(0K)}|4\rangle, \end{aligned}$$

where we notice that $\omega_{24} - \omega_{13} = \Delta\epsilon_Z/\hbar$ is the tunneling frequency mismatch, and $R_{4224}(\omega_{24}) + R_{3113}(\omega_{13}) = \bar{\Gamma}/\pi$, with $\bar{\Gamma}$ being the average tunneling rate. The sum of spectral densities in the first equation, $R_{1342}(\omega_{24}) + R_{1342}(\omega_{13}) \equiv \tilde{\Gamma}/\pi$, may be expected to be of similar value, i.e. we assume that $\tilde{\Gamma} \approx \bar{\Gamma}$. We deal then with an exponential spin coherence outflow from QD2 taking place during tunneling, while the related inflow to QD1 is affected by a phase factor oscillating with frequency equal to $\Delta\epsilon_Z/\hbar$, resulting from the fact that the transfer takes place between coherences oscillating with such a frequency mismatch inherited from the Larmor precession of spins. The solution for the total spin coherence in the case of the equal initial spin superposition is

$$C(t) \simeq \frac{1}{2} \left[\frac{1}{1 - i\frac{\Delta\epsilon_Z}{\hbar\bar{\Gamma}}} \left(1 - e^{i\frac{\Delta\epsilon_Z}{\hbar}t - \bar{\Gamma}t} \right) + e^{-\bar{\Gamma}t} \right],$$

where, apart from oscillations, a term in the denominator responsible for reducing the inflow part is present. Calculating the asymptotic value, we find a formula for the preserved coherence,

$$C(\infty) \simeq \frac{1}{1 - i\frac{\Delta\epsilon_Z}{\hbar\bar{\Gamma}}} \simeq \frac{1}{\sqrt{\tau_+\tau_- \left[\left(\frac{2\Delta\epsilon_Z}{\hbar} \right)^2 + \left(\frac{1}{\tau_+} + \frac{1}{\tau_-} \right)^2 \right]}},$$

which is identical as the one derived within the theory of spontaneous emission in Sec. AIII.

Next, we return to equations (A4) and focus only on terms that arise at $T > 0$ K, namely

$$\begin{aligned} \langle 1|\dot{\rho}_e|2\rangle &\simeq \langle 1|\dot{\rho}_e|2\rangle \Big|_{T=0K} \\ &\quad - \pi \left[e^{-\frac{\hbar\omega_{24}}{kT}} R_{4224}(\omega_{24}) + e^{-\frac{\hbar\omega_{13}}{kT}} R_{3113}(\omega_{13}) \right] \langle 1|\rho_e|2\rangle, \\ \langle 3|\dot{\rho}_e|4\rangle &\simeq \langle 3|\dot{\rho}_e|4\rangle \Big|_{T=0K} + \pi e^{-i\frac{\Delta\epsilon_Z}{\hbar}t} \\ &\quad \times \left[e^{-\frac{\hbar\omega_{24}}{kT}} R_{3124}(\omega_{24}) + e^{-\frac{\hbar\omega_{13}}{kT}} R_{3124}(\omega_{13}) \right] \langle 1|\rho_e|2\rangle. \end{aligned}$$

In the first equation, we now see the damping of the ground-state spin coherence $\langle 1|\rho_e|2\rangle$ with a rate proportional to the rate of thermally activated tunneling to the higher energy dot. The approximate rate of this process, and hence of associated spin decoherence is

$$\Gamma_{\text{virt}} = \frac{1}{2} \left(e^{-\frac{\hbar\omega_{24}}{kT}} \Gamma_+ + e^{-\frac{\hbar\omega_{13}}{kT}} \Gamma_- \right) \simeq \bar{\Gamma} e^{-\frac{\Delta\epsilon_0}{kT}},$$

so, for long enough times (after a few tunneling times), at which the dynamics governed by $\langle i|\dot{\rho}_e|j\rangle \Big|_{T=0K}$ is already at equilibrium, we deal with a thermally activated exponential coherence loss. In Fig. A2 we present numerically simulated time evolution of spin coherence for structure S22 at various temperatures (solid lines) along with the electron localization (dashed lines). One may notice that at low temperatures the two processes take place at well-resolved timescales, while at $T > 25$ K the virtual tunneling becomes effective enough to coincide with the real process. This is the reason for the deviation of numerically estimated decoherence times from expected exponential tendency at higher temperatures, which may be found in Fig. 5.

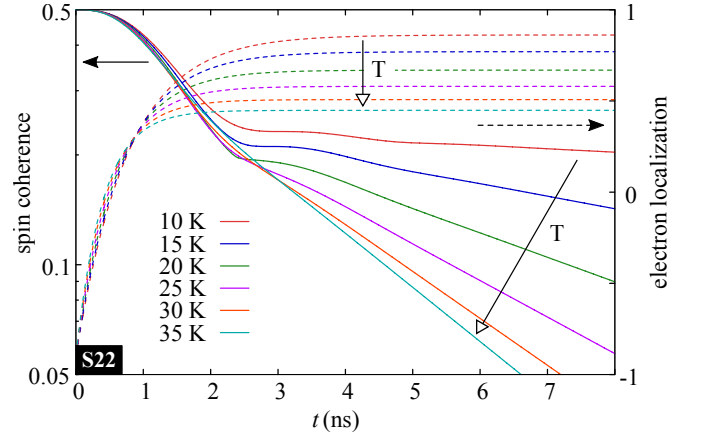


FIG. A2: (Color online) Evolution of spin coherence for structure S22 at various temperatures (solid lines, left axis) and corresponding electron localization (dashed lines, right axis). Open-headed arrows indicate the direction of rising temperature for each set of lines.

¹ T. Nakaoka, T. Saito, J. Tatebayashi, and Y. Arakawa, Phys. Rev. B **70**, 235337 (2004).

² J. van Bree, A. Y. Silov, P. M. Koenraad, M. E. Flatté, and C. E. Pryor, Phys. Rev. B **85**, 165323 (2012).

³ I. Vurgaftman, J. R. Meyer, and L. R. Ram-Mohan, Journal of Applied Physics **89**, 5815 (2001).

⁴ V. Weisskopf and E. Wigner, Zeitschrift für Physik **63**, 54

(1930).

⁵ M. O. Scully and M. S. Zubairy, *Quantum Optics* (Cambridge University Press, 1997).

⁶ K. Roszak, A. Grodecka, P. Machnikowski, and T. Kuhn, Phys. Rev. B **71**, 195333 (2005).